UNCLASSIFIED

AD 295 751

Reproduced
by the

ARMED SERVICES TECHNICAL INFORMATION AGENCY
ARLINGTON HALL STATION
ARLINGTON 12, VIRGINIA

UNCLASSIFIED

NOTICE: When government or other drawings, specifications or other data are used for any purpose other than in connection with a definitely related government procurement operation, the U. S. Government thereby incurs no responsibility, nor any obligation whatsoever; and the fact that the Government may have formulated, furnished, or in any way supplied the said drawings, specifications, or other data is not to be regarded by implication or otherwise as in any manner licensing the holder or any other person or corporation, or conveying any rights or permission to manufacture, use or sell any patented invention that may in any way be related thereto.

63-2-3

CATALOGED BY ASTIA
AS AD No. 295751
295 751

OFFICE OF NAVAL RESEARCH

Contract Nonr 562(10)

NR-064-406

Technical Report No. 85

LINERIZATION IN PROBLEMS OF FINITE PLASTIC FLOW

by

Manohar Singh

DIVISION OF APPLIED MATHEMATICS

BROWN UNIVERSITY

PROVIDENCE, R. I.

January 1963

C11-85

ASTIA
FEB 6 1963
TISIA

Reproduction in whole or in part is permitted for any purpose of the United States Government.

Abstract

Various methods of linearising yield condition and flow rule are discussed in connection with problems in finite plastic strains (drawing of tubes, nosing of shells). The numerical results presented in this paper show that, when carefully handled, some of these methods give excellent approximations to the predictions of von Mises theory, which will usually involve more elaborate analysis.

Linearization in Problems of Finite Plastic Flow

By Manohar Singh (Brown University)

1. Introduction

The oldest yield condition in the theory of plasticity is that of Tresca [1]**. When the principal stresses are used as rectangular co-ordinates in a three-dimensional stress space, it is represented by a regular hexagonal prism. As long as the variations of stress in a problem are such that the stress point remains restricted to one face of this prism, the linear character of the yield condition greatly simplifies the mathematical analysis. The complications that arise when several faces must be considered in the solution of a problem induced von Mises [2] to suggest that the prism be approximated by the inscribed circular cylinder. Later experiments showed that the resulting non-linear yield condition, which was introduced for mathematical convenience, actually describes the behaviour of plastic metals better than the piecewise linear yield condition of Tresca. On the other hand, the hope that a single non-linear expression would be less unwieldy than six linear expressions

* The results communicated in this paper were obtained in the course of research sponsored by the Office of Naval Research under Contract Nonr 562(10) with Brown University.

** Numbers in square brackets refer to the Bibliography at the end of the paper.

did not, on the whole, prove justified, and linearised yield conditions have been used in the solution of many problems in plasticity.

In the early stages of plasticity, yield condition and flow rule were viewed as independent components of the theory, and investigators felt free to use the flow rule of Saint Venant and Levy [3] with whatever yield condition proved convenient in the solution of a problem. Recent work on limit analysis, however, has suggested the connection between yield condition and flow rule that is expressed by the principle of maximum plastic dissipation [4]. If this principle is accepted, linearisation of the yield condition should be accompanied by a change in flow rule that maintains the validity of this principle. While this "joint linearisation of yield condition and flow rule" has been widely used in limit analysis and design [5], relatively few problems of finite plastic flow have been treated in this manner. In this paper, some problems of this kind will be solved for a material obeying the yield condition of von Mises and the flow rule of Saint Venant and Levy, and the solutions will be compared to those obtained by various joint linearisations of yield condition and flow rule.

PART I. Drawing of thin-walled tube through a conical die.

2. The problem.

In considering the drawing of a rigid, perfectly plastic thin-walled tube through a well-lubricated conical die (Fig. 1), we shall restrict the discussion to the steady state of plastic flow and assume that the wall thickness is small in comparison to the length of contact with the die. The variation of stress across the thickness of the wall will therefore be neglected. On account of the rotational symmetry of the problem and the absence of shearing stresses between tube and die, the normals to the meridional planes and to the die surface indicate principal directions of stress.

Subject to later confirmation by the numerical results, it will be assumed that the normal pressure p between the tube and die is small in comparison to the meridional stress σ_1 or the circumferential stress σ_2, so that a yield condition for plane stress and the corresponding flow rule will be appropriate. Since several yield conditions will be used, we shall establish the basic equations for an arbitrary yield condition written as

$$F(\sigma_1,\sigma_2) = 0. \tag{2.1}$$

In view of the rotational symmetry of the problem, and since the variations of σ_1 and σ_2 across the wall thickness are neglected, these principal stresses depend only on the distance s measured along the die. With the notations in Fig. 1, equilibrium in the meridional direction requires that

$$\frac{d}{ds}(\sigma_1 hr) + \sigma_2 h \sin\alpha = 0. \tag{2.2}$$

Since

$$s = \frac{a-r}{\sin\alpha}, \tag{2.3}$$

we may alternatively consider σ_1, σ_2 and h as functions of r to write (2.2) in the form

$$\frac{r}{h}\frac{dh}{dr}\sigma_1 + r\frac{d\sigma_1}{dr} + (\sigma_1 - \sigma_2) = 0. \tag{2.4}$$

Since the considered rigid, perfectly plastic material lacks viscosity, the "time" used in the definition of the strain rates may be any quantity that increases monotonically during the motion of the typical particle along the die. We take this quantity to be -r and denote by v the radial "velocity" component of the particle. The "strain rates" in the meridional, circumferential, and thickness directions are then given by

$$\dot{\varepsilon}_1 = -\frac{dv}{dr}\ ;\ \dot{\varepsilon}_2 = -\frac{v}{r}\ ;\ \dot{\varepsilon}_3 = \frac{dh/dt}{h} = -\frac{vdh}{hdr}\ . \tag{2.5}$$

No comments are needed regarding the first two relations (2.5). In deriving the last, use has been made of the facts that the flow is stationary ($\partial h/\partial t = 0$) and that the "velocity" v has been defined with respect to the "time" -r. As is customary in the theory of plasticity, the material will be treated as incompressible. The incompressibility condition $\dot{\varepsilon}_1 + \dot{\varepsilon}_2 + \dot{\varepsilon}_3 = 0$ and the relations (2.5) furnish

$$\frac{v}{h}\frac{dh}{dr} + \frac{dv}{dr} + \frac{v}{r} = 0. \tag{2.6}$$

Finally, the flow rule implied by the principal of maximum plastic dissipation requires that

$$\dot{\varepsilon}_1 = \lambda \frac{\partial F}{\partial \sigma_1} \; ; \; \dot{\varepsilon}_2 = \lambda \frac{\partial F}{\partial \sigma_2} , \tag{2.7}$$

wherever the yield function F is continuously differentiable. The co-efficient of proportionality λ in (2.7) is non-negative; it is not a characteristic constant of the material but a parameter that must be eliminated from the equations.

The boundary conditions for the problem under consideration are

$$\sigma_1 = 0 \; , \; h = h_o , \; v = v_o \quad \text{for } r=a=1. \tag{2.8}$$

We are now in a position to consider various yield conditions.

3. Yield condition of von Mises.

For plane stress, the yield condition of von Mises takes the form

$$F \equiv \sigma_1^2 - \sigma_1\sigma_2 + \sigma_2^2 - \sigma_o^2 = 0 , \tag{3.1}$$

where σ_o is the yield stress in simple tension. Equation (3.1) may be re-written as

$$F \equiv (2\sigma_2-\sigma_1)^2 + 3\sigma_1^2 - 4\sigma_o^2 = 0. \tag{3.2}$$

With the use of (3.1) and (2.5), the flow rule (2.7) furnishes

$$\frac{dv}{dr} = \frac{2\sigma_1-\sigma_2}{2\sigma_2-\sigma_1}\,\frac{v}{r} . \tag{3.3}$$

It follows from (3.3) and (2.6) that

$$\frac{r}{h}\frac{dh}{dr} = -\frac{\sigma_1+\sigma_2}{2\sigma_2-\sigma_1} \tag{3.4}$$

Equations (2.4), (3.2) and (3.4) constitute a system with three unknown functions of r, namely σ_1, σ_2, and h.

Stresses. Substituting from (3.4) into (2.4), one finds the relation

$$r\frac{d\sigma_1}{dr} = \frac{2\sigma_o^2}{2\sigma_2-\sigma_1}, \tag{3.5}$$

which, on using (3.2), becomes

$$r\frac{d\sigma_1}{dr} = \pm\frac{2\sigma_o^2}{[4\sigma_o^2-3\sigma_1^2]^{\frac{1}{2}}}. \tag{3.6}$$

In the stress space with the rectangular Cartesian coordinates σ_1,σ_2, equation (3.1) is represented by an ellipse (Fig. 2a). The point A corresponds to the state of stress at the die entrance where $\sigma_1 = 0$ and $\sigma_2 < 0$, and the point B corresponds to the die exit. The position of the point B is restricted to the arc AA'. Indeed, at A', the tangent to the yield ellipse F=0 is parallel to σ_2-axis, so that $(\partial F/\partial\sigma_1)/(\partial F/\partial\sigma_2) = \dot{\varepsilon}_1/\dot{\varepsilon}_2$ becomes infinite. Since $\dot{\varepsilon}_2 = -\frac{v}{r}$ cannot vanish if the tube is to move through the die, this means that $\dot{\varepsilon}_1$ would have to be infinite, so that the neglection of strain rate effects would no longer be justified as the stress point approaches A'.

Since $2\sigma_2-\sigma_1 < 0$ on the arc AA', equation (3.5) shows $r\, d\sigma_1/dr$ to be negative. Accordingly, the minus sign applies in (3.6). Integrating this differential equation for σ_1 and using the boundary condition $\sigma_1=0$ for $r=a=1$, we obtain

$$\frac{1}{2}\frac{\sigma_1}{\sigma_o}\left[1-\frac{3}{4}\left(\frac{\sigma_1}{\sigma_o}\right)^2\right]^{\frac{1}{2}}+\frac{1}{3^{\frac{1}{2}}}\text{arc}\sin\left(\frac{3^{\frac{1}{2}}}{2}\frac{\sigma_1}{\sigma_o}\right)=\log\frac{1}{r}\,. \tag{3.7}$$

This equation specifies the radius r at which a given value of σ_1/σ_o occurs, and the yield condition (3.2) gives the corresponding value of σ_2/σ_o as

$$\frac{\sigma_2}{\sigma_o}=\frac{1}{2}\frac{\sigma_1}{\sigma_o}-\left[1-\frac{3}{4}\left(\frac{\sigma_1}{\sigma_o}\right)^2\right]^{\frac{1}{2}}\,. \tag{3.8}$$

Note that the plots of σ_1/σ_o and σ_2/σ_o versus r (heavy lines in Figs. 3 and 4) are independent of the exit radius b of the die.

We now examine the limit set for the value of the exit radius b by the fact that the stress point in Fig. 2b should remain on the arc AA'. At A', where $2\sigma_2-\sigma_1=0$, equation (3.2) shows σ_1/σ_o to have the value $\frac{2}{3^{\frac{1}{2}}}=1.15470$. Substituting this value into (3.7), we obtain $r=0.40377$. The present analysis therefore requires that the exit radius b of the die be larger than 0.40377.

<u>Thickness Changes</u>. Substituting from (3.6) into (3.4) and integrating under the boundary condition $h=h_o$, $\sigma_1=0$, for $r=a=1$, we obtain

$$\log\frac{h}{h_o}=-\frac{1}{4}\left[\frac{3}{2}\left(\frac{\sigma_1}{\sigma_o}\right)^2+2\log r\right]. \tag{3.9}$$

<u>Velocity Distribution</u>. Substituting for dr/r from (3.6) and σ_2 from (3.8) into (3.3), we find

$$\frac{dv}{v} = [\tfrac{3}{4}\,\sigma_1 + \tfrac{1}{4}(4\sigma_o^2 - 3\sigma_1^2)^{\frac{1}{2}}]d\sigma_1 \; . \qquad (3.10)$$

Integration of (3.10) under the boundary condition $v=v_o$, $\sigma_1=0$ for $r=a=1$ yields

$$\log(v/v_o) = \tfrac{3}{8}(\sigma_1/\sigma_o)^2 - \tfrac{1}{2}\log r \; . \qquad (3.11)$$

It is of interest to note that h/h_o and v/v_o plotted versus r in Figs. 5 and 6 respectively (heavy lines) depend also on the meridional stress σ_1/σ_o.

4. Linearised yield condition.

In treating the problem under discussion, Swift [6] used the linear yield condition of Tresca [1] in conjunction with the flow rule of Saint Venant and von Mises [7]. This, however, does not significantly simplify the analysis presented above. Prager [8] then pointed out that the problem could be solved in closed form if the linear yield condition was combined with the flow rule associated with it by the principle of maximum plastic dissipation [4]. While this simultaneous linearisation of yield condition and flow rule gives good results as far as the stresses are concerned, Sokolovskii [9] drew attention to the fact that it does not furnish thickness changes that agree well with those predicted by the yield condition of von Mises and the flow rule of Saint Venant and Levy.

Since we may find it desirable to replace the elliptic arc AB in Fig. 2a by one or more straight segments, we formulate the linearised treatment in some generality.

Let $L(\sigma_1', \sigma_2')$ and $M(\sigma_1'', \sigma_2'')$ be two arbitrary points on the yield ellipse (Fig. 2a). The line LM has the equation

$$F \equiv m(\sigma_1 - \sigma_1') - (\sigma_2 - \sigma_2') = 0 , \tag{4.1}$$

where $m = (\sigma_2'' - \sigma_2')/(\sigma_1'' - \sigma_1')$. According to the yield condition (4.1), the flow rule (2.7) furnishes

$$\dot{\varepsilon}_1/\dot{\varepsilon}_2 = (dv/dr)/(v/r) = -m . \tag{4.2}$$

The equation of incompressibility (2.6) now reduces to

$$\frac{rdh}{hdr} = -(1-m). \tag{4.3}$$

The set of three equations (2.4), (4.1) and (4.3) are the governing equations of the linearised treatment of our problem. Substituting from (4.1) and (4.3) into (2.4), we obtain

$$d\sigma_1 = (\sigma_2' - m\sigma_1') \frac{dr}{r} . \tag{4.4}$$

Remembering that at the point L, $\sigma_1 = \sigma_1'$ and $\sigma_2 = \sigma_2'$, and denoting the values of r, v and h at this point by r', v' and h', we integrate (4.2), (4.3) and (4.4) to find

$$\frac{v}{v'} = \left(\frac{r'}{r}\right)^m , \tag{4.5}$$

$$\frac{h}{h'} = \left(\frac{r'}{r}\right)^{1-m} , \tag{4.6}$$

$$\sigma_1 = \sigma_1' + (\sigma_2' - m\sigma_1') \log \frac{r}{r'} . \tag{4.7}$$

Substitution of (4.7) into the linearised yield condition (4.1) finally furnishes

$$\sigma_2 = \sigma_2' + m(\sigma_2' - m\sigma_1') \log \frac{r}{r'} . \tag{4.8}$$

5. Single linear yield condition.

Since the radius of the die exit has to be larger than 0.40377, let us consider $b = 0.405$. In place of the elliptic arc AB, we shall consider the straight segment LM as the yield locus (Fig. 2b). As $\sigma_1 = 0$, and $\sigma_2 < 0$ when $r = a = 1$, the point L must coincide with A, whereas the position of B on the linear yield locus is not known at this stage. With the help of the boundary conditions (2.8), the equations (4.5) through (4.8) reduce to

$$v/v_o = 1/r \ ,$$
$$h/h_o = 1 \ ,$$
$$\sigma_1/\sigma_o = -\log r \ ,$$
$$\sigma_2/\sigma_o = -(1+\log r) \, .$$

The meridional stress σ_1/σ_o obtained through the above procedure agrees sufficiently well with that of the theory of von Mises (Fig. 3). The thickness h/h_o, circumferential stress σ_2/σ_o, and velocity v/v_o are more at variance (Figs. 4, 5 and 6).

6. Two or more linear yield conditions.

In trying to improve our results, we may approximate the elliptic arc AB by more than one straight line so as to stay closer to the arc. In the problem at hand, we may take the straight line segments LM', M'M and if necessary MA' (Fig. 2b), where

$$\sigma_1(M') = 0.5\sigma_o \ ; \ \sigma_1(M) = \sigma_o \ ; \ \sigma_1(A') = 1.1547\sigma_o \ .$$

Substituting m = 0.69722 for the slope of LM' into equations (4.5) through (4.8), we obtain

$$\frac{v}{v_o} = \left(\frac{1}{r}\right)^{0.69722} , \tag{6.1}$$

$$\frac{h}{h_o} = \left(\frac{1}{r}\right)^{0.30278} , \tag{6.2}$$

$$\frac{\sigma_1}{\sigma_o} = -\log r , \tag{6.3}$$

$$\frac{\sigma_2}{\sigma_o} = -0.30278 \log r . \tag{6.4}$$

Since $\frac{\sigma_1}{\sigma_o}(M') = 0.5$, the equation (6.3) gives $r(M') = 0.60653$. The first linear yield locus, therefore covers the range $1 \geq r \geq 0.60653$.

The next segment of the tube either corresponds to a fixed state of stress at M' and strain rate vectors that vary between the normal to LM' and the normal to M'M, or the next segment corresponds to the line M'M. The first situation cannot arise, because the equilibrium equation (2.4) can be re-written as

$$r \frac{d\sigma_1}{dr} - \left(1 + \frac{\dot{\varepsilon}_1}{\dot{\varepsilon}_2}\right)\sigma_1 + (\sigma_1 - \sigma_2) = 0 ,$$

and if σ_1 and σ_2 were constant, the ratio $\dot{\varepsilon}_1/\dot{\varepsilon}_2$ would also have to be constant in contradiction to the assumption of varying direction of the strain rate vector.

If we think of the point M' as having the coordinates σ_1', σ_2', the formulas (4.5) through (4.8) apply on the two sides of this point with different values of the slope m. This shows that we can make v, h, σ_1, and σ_2 behave in a continuous manner as we go from one segment to the next. Since v is continuous, $\dot{\varepsilon}_2 = -v/r$ is also continuous, but $\dot{\varepsilon}_1 = -dv/dr$ and $\dot{\varepsilon}_3 = -(v/h)dh/dr$ are not. These discontinuities, however, are permissible.

The line M'M has the slope 1.30278, so that formulas (4.4) through (4.8) yield

$$v/v_{M'} = [(0.60653/r]^{1.30278} , \tag{6.5}$$

$$h/h_{M'} = [(0.60653)/r]^{-0.30278} , \tag{6.6}$$

$$\sigma_1/\sigma_o = 0.5 - (1.30278) \log \frac{r}{0.60653} , \tag{6.7}$$

$$\sigma_2/\sigma_o = -0.65139 - (1.30278)^2 \log \frac{r}{0.60653} \tag{6.8}$$

for $0.60653 \geq r \geq r(M)$. Substituting for $\sigma_1/\sigma_o = 1$ in equation (6.7), we find

$$r(M) = 0.41321.$$

For values of $r < 0.41321$, we continue the above procedure along the line MA'. Proceeding in a similar manner, one obtains

$$r(A') = 0.39643$$

so that the point B corresponding to $r = 0.405$ falls on the segment MA'. The quantities σ_1/σ_o , σ_2/σ_o , h/h_o , and v/v_o as obtained from the above process of three linear yield conditions are plotted in Figures 3, 4, 7 and 8 respectively.

Since the linearised treatment developed above gives satisfactory results for σ_1 (Fig. 3), we can obtain better approximations for σ_2 by substituting σ_1 into (3.1). We may also try to improve v and h by substituting the stresses from the linearised theory into the differential equations (3.3) and (3.4) of the von Mises theory, as is discussed in the following section.

7. Modified linearised procedure.

Substituting (4.7) and (4.8) into (3.4) and then integrating, we obtain

$$\log \frac{h}{h'} =$$

$$\frac{1+m}{1-2m}\left[\log(r/r') + \frac{3}{(1+m)(1-2m)} \log\left\{1 - \frac{(1-2m)(\sigma_2'-m\sigma_1')}{2\sigma_2'-\sigma_1'} \log \frac{r}{r'}\right\}\right]. \tag{7.1}$$

Where h=h' when r=r'.

Substitution of σ_1/σ_o and σ_2/σ_o from (4.7) and (4.8) into (3.3) and integration of the resulting equations furnishes

$$\log \frac{v}{v'} =$$

$$\frac{2-m}{2m-1}\left[\log(r/r') + \frac{3}{(1-2m)(2-m)} \log\left\{1 - \frac{(1-2m)(\sigma_2'-m\sigma_1')}{2\sigma_2'-\sigma_1'} \log \frac{r}{r'}\right\}\right]. \tag{7.2}$$

Where v=v' when r=r'.

Finally, with the aid of (7.1), equation (7.2) can be put in the simple form

$$v/v' = 1/(r/r')(h/h'). \tag{7.3}$$

<u>Single Linear Yield Condition</u>. When the yield locus is the segment LM in Fig.(2b), on using the boundary condition, the equations (7.1) and (7.3) give

$$\log \frac{h}{h_o} = -2[\log r - \frac{3}{2} \log(1 + \frac{1}{2} \log r)] \tag{7.4}$$

and

$$\frac{v}{v_o} = 1/(rh)/h_o. \tag{7.5}$$

The curves h/h_o and v/v_o versus r given by (7.4) and (7.5) are shown in Figs. 5 and 6 respectively.

<u>Two or More Linear Yield Conditions (Fig. 2b)</u>. When the yield locus consists of straight segments LM', M'M and MA' (§5), we have along LM' (for $1 \geq r \geq 0.60653$):

$$m = 0.69722, \quad \sigma_1' = 0, \quad \sigma_2' = -\sigma_o, \quad r' = 1, \quad h' = h_o, \quad v' = v_o$$

along M'M (for $0.60653 \geq r \geq 0.41321$):

$$m = 1.30278, \ \sigma_1' = 0.5\sigma_o, \quad \sigma_2' = -0.65139, \ r' = 0.60653,$$
$$h' = (h)_{M'}, \quad v' = (v)_{M'}$$

along MA' (for $0.41321 \geq r > 0.36695$):

$$m = 3.73206, \quad \sigma_1' = \sigma_o, \quad \sigma_2' = 0, \quad r' = 0.41321,$$
$$h' = (h)_M, \quad v' = (v)_M.$$

The equations (7.1) and (7.3) with the help of above data provide us the curves h/h_o and v/v_o versus $r(0.405 \leq r \leq 1)$ plotted in Figs. 7 and 8. It is clear from the comparison of graphs in Figs. 5-8 that the deformations h/h_o, velocities v/v_o

obtained through the above modified procedure of using linearised stresses in von Mises flow rule are in almost complete agreement with those obtained from von Mises theory directly.

For smaller drawing such as b=0.7, only one linear yield locus LM' (Fig. 2b) should be appropriate. The Figures 3, 4, 7 and 8 exhibit clearly that in such a case both the linearised procedure and the modified linearised procedure give excellent results.

PART II. The Nosing of Shells.

8. Basic relations.

Consider the forming of an ogive nose at the end of a tubular part by pressing the tube into a well lubricated suitably formed die (Fig.9a). Using Tresca's yield condition and the corresponding flow rule, Onat and Prager [10] analysed the stresses and changes in wall thickness. The present discussion will be restricted to moderate degrees of penetration of the tube into the die, and the wall thickness will be treated as small in comparison to the radius of the tube so that the variation of stress across the thickness may be neglected. As in Part I, the meridional and circumferential stresses σ_1 and σ_2 far exceed the normal pressure p, and the problem can therefore be treated as one in plane stress with σ_1 and σ_2 as the principal stresses.

Consider a shell element of the wall thickness h and the radius $r = R \cos \varphi - a$ (for notations, see Fig.9a). The equilibrium requirement furnishes the equation,

$$\frac{d}{dr}(h\sigma_1) + \frac{h}{r}(\sigma_1 - \sigma_2) = 0. \tag{8.1}$$

Writing the yield condition as

$$f(\sigma_1, \sigma_2) = 0, \tag{8.2}$$

we use the flow rule

$$\dot{\varepsilon}_1 = \lambda \frac{\partial f}{\partial \sigma_1} ; \quad \dot{\varepsilon}_2 = \lambda \frac{\partial f}{\partial \sigma_2} . \qquad (\lambda \geq 0) \tag{8.3}$$

As before, the equation of incompressibility gives

$$\frac{v}{h}\frac{dh}{dr} + \frac{dv}{dr} + \frac{v}{r} = 0 \tag{8.4}$$

These equations must be solved subject to the boundary conditions

$$\sigma_1 = 0 \quad \text{for } \varphi = \varphi_1 \quad \text{i.e. } r = r_1, \tag{8.5}$$

$$v = v_o, h = h_o, \quad \text{for } \varphi = 0 \quad \text{i.e. } r = a = 1. \tag{8.6}$$

Except for the boundary conditions, the problem is therefore quite similar to that of Part I, so that we may apply the procedure of Part I to the present problem.

9. <u>von Mises yield condition.</u>

For plane stress, yield condition of v.Mises is given by

$$f \equiv \sigma_1^2 - \sigma_1\sigma_2 + \sigma_2^2 - \sigma_o^2 = 0, \tag{9.1}$$

where σ_o is the yield stress in simple tension. The flow rule gives

$$\dot{\varepsilon}_1/\dot{\varepsilon}_2 = (-dv/dr)/(-v/r) = (2\sigma_1-\sigma_2)/(2\sigma_2-\sigma_1) \tag{9.2}$$

In the stress space with the rectangular cartesian co-ordinates σ_1 and σ_2, the equation (9.1) represents an ellipse, and the point A representing the state of stress $\sigma_1=0$, $\sigma_2 < 0$ at the free end of the nose of the shell lies on the σ_2 axis (Fig.9b). Once again the position of the point B which represents the stress state at the die entrance r=a=1 is confined to the arc AA' of the yield ellipse (Fig.9b), because at A', the tangent is parallel to the σ_2 axis (see the discussion in Section 3). The equations (8.1), (8.4), (9.1) and (9.2) with the boundary conditions (8.5) and (8.6), furnish the solution

$$\frac{1}{2}\frac{\sigma_1}{\sigma_o}\left[1-\frac{3}{4}\left(\frac{\sigma_1}{\sigma_o}\right)^2\right]^{\frac{1}{2}}+\frac{1}{3^{\frac{1}{2}}}\arcsin\left(\frac{3^{\frac{1}{2}}}{2}\frac{\sigma_1}{\sigma_o}\right)=\log\frac{r_1}{r}, \tag{9.3}$$

$$\frac{\sigma_2}{\sigma_o}=\frac{1}{2}\frac{\sigma_1}{\sigma_o}-\left[1-\frac{3}{4}\left(\frac{\sigma_1}{\sigma_o}\right)^2\right]^{\frac{1}{2}}, \tag{9.4}$$

$$\log\frac{h}{h_o}=-\frac{1}{4}\left[\frac{3}{2}\left(\frac{\sigma_1}{\sigma_o}\right)^2-\frac{3}{2}\left(\frac{\sigma_1}{\sigma_o}\right)^2_{\text{at } r=1}+2\log r\right], \tag{9.5}$$

$$\log\frac{v}{v_o}=\frac{3}{8}\left(\frac{\sigma_1}{\sigma_o}\right)^2-\frac{3}{8}\left(\frac{\sigma_1}{\sigma_o}\right)^2_{\text{at } r=1}-\frac{1}{2}\log r=-\log\left(r\frac{h}{h_o}\right). \tag{9.6}$$

It should be noted here that unlike the problem in Part I, all the quantities σ_1, σ_2, h, and v in this problem depend upon r_1, the degree of penetration of the tube into the die.

The fact that the point B is restricted to the arc AA' implies that for r=1, the ratio $\left|\frac{\sigma_1}{\sigma_o}\right|$ has the maximum value 1.15470. Substituting this in (9.3), we obtain $r_1 = 0.40377$. Thus, for the present analysis to be valid, r_1 must be greater than 0.40377, that is $\varphi_1 = \arccos\left(\frac{1+r_1}{2}\right)$ must be less than 0.79275.

In particular, let us consider $\varphi_1=0.75$ so that $r_1 = 0.46337$. The quantities σ_1/σ_o, σ_2/σ_o, h/h_o, and v/v_o as evaluated from equations (9.3) through (9.6), are shown as functions of r by the heavy lines in Figures 10, 11, 12, and 13, respectively.

10. Single linear yield condition.

We now approximate the elliptic arc AB by a single straight segment LM (Fig.9b). The point L which represents the state of stress at the free end of the tube coincides with A, whereas the position of B on the linear yield locus LM is not known at this stage. The line LM has the slope m=0. With the use of the boundary conditions (8.5) and (8.6), the equations (4.5) through (4.8) yield

$$v/v_o = (h_o)/(rh) = 1 \ , \tag{10.1}$$

$$h/h_o = 1/r \ , \tag{10.2}$$

$$\sigma_1/\sigma_o = -\log(r/r_1) \ , \tag{10.3}$$

$$\sigma_2/\sigma_o = -1 \ . \tag{10.4}$$

Setting $\sigma_1/\sigma_o = -1$ in (10.3), one finds

$$r(M) = 1.25958,$$

so that $r(B) = 1$ lies on the segment LM. The plots of σ_1/σ_o, σ_2/σ_o, h/h_o, and v/v_o as functions of r are shown in Figures 10, 11, 12, and 13, respectively.

11. Two linear yield conditions.

To improve the results, we replace the elliptic arc AB by two straight line segments LM', and M'M. To stay close to the relevant arc of the yield locus, we choose the point M' at the lowest point of the ellipse (Fig.9b), where $\sigma_1(M')=-0.57735\sigma_o$ and $\sigma_2(M')=-1.15470\sigma_o$. Accordingly, the line LM' has the slope

$m = 0.26795$ and the line M'M the slope $m' = -0.36602$. With the aid of (8.5) and (8.6), the equations (4.5) through (4.8) now yield

$$v/v_o = (r')^{m-m'}/(r)^m \quad , \tag{11.1}$$

$$h/h_o = (r')^{m'-m}/(r)^{1-m} \, , \tag{11.2}$$

$$\sigma_1/\sigma_o = -\log(r/r_1) \quad , \tag{11.3}$$

$$\sigma_2/\sigma_o = -1-m \log(r/r_1) \quad . \tag{11.4}$$

The equation (11.3) gives $r(M') = r' = 0.82541$. This set of formulas is valid in the range $0.46337 \leq r \leq 0.82541$. Along M'M, we find

$$v/v_o = (1/r)^{m'} \, , \tag{11.5}$$

$$h/h_o = (1/r)^{1-m'}, \tag{11.6}$$

$$\sigma_1/\sigma_o = -0.57735 + (m'-2)/3^{\frac{1}{2}} \log(r/r') \, , \tag{11.7}$$

$$\sigma_2/\sigma_o = -1.15470 + \frac{1}{2} \log(r/r') \, . \tag{11.8}$$

Substituting -1 for σ_2/σ_o in (11.8), we obtain

$$r(M) = 1.12470.$$

The point $B(r=1)$ thus lies on the segment M'M.

12. Modified linearised procedure.

The comparison of Fig. 10 with Figures 11 through 15 shows again that the process of linearisation gives the stress σ_1 in good agreement with that of the von Mises theory, the stress σ_2, the thickness h and the velocity v still could be improved. To achieve this, we apply the procedure of Section 7, substituting σ_1 into (9.1) to obtain σ_2, and putting the stresses from the linearised theory into the differential equations (3.3) and (3.4) to get

$$\log \frac{h}{h'} = \frac{1+m}{1-2m}\left[\log(r/r') + \frac{3}{(1+m)(1-2m)} \log\left\{1 - \frac{(1-2m)(\sigma_2'-m\sigma_1')}{2\sigma_2'-\sigma_1'} \log(r/r')\right\}\right], \tag{12.1}$$

and

$$v/v' = 1/(r/r')(h/h'), \tag{12.2}$$

where $h=h'$, $v=v'$ when $r=r'$.

<u>Single Linear Yield Condition</u>: Since the slope m of the line LM (Fig.9b) is zero, equation (12.1) gives

$$\log(h/h_1) = [\log(r/r_1) + 3 \log(1 - \tfrac{1}{2} \log r/r_1)]. \tag{12.3}$$

With the use of the boundary condition (8.6), equations (12.2) and (12.3) reduce to

$$\log(h/h_o) = \log r + 3 \log(1 - \frac{\log r}{2+\log r_1}) \tag{12.4}$$

and

$$v/v_o = (h_o)/(rh). \tag{12.5}$$

The values of h/h_o and v/v_o so obtained are plotted in Figs. 12 and 13.

<u>Two Linear Yield Conditions. (Fig.9b)</u>: Along the line LM', whose slope m is 0.26795, equations (12.1) and (12.2) yield

$$\log \frac{h}{h'} =$$

$$\frac{1+m}{1-2m}\left[\log \frac{r}{r'} + \frac{3}{(1+m)(1-2m)} \log\left\{1 - \frac{(1-2m)(2-m)}{3} \log \frac{r}{r'}\right\}\right], \quad (12.6)$$

$$v/v_o = (h_o)/(rh) \quad (12.7)$$

for the range $0.46337 \leq r \leq 0.82541$, whereas along the line M'M with the slope $m' = -0.36602$, we have

$$\log \frac{h}{h'} =$$

$$\frac{1+m'}{1-2m'}\left[\log \frac{r}{r'} + \frac{3}{(1+m')(1-2m')} \log\left\{1 - \frac{(1-2m')(2-m')}{3} \log \frac{r}{r'}\right\}\right], \quad (12.8)$$

$$v/v_o = (h_o)/(rh) \quad (12.9)$$

for the range $0.82541 \leq r \leq 1$.

From (12.8) and (8.6), it follows

$$\log \frac{h_o}{h'} =$$

$$\frac{1+m'}{1-2m'}\left[-\log r' + \frac{3}{(1+m')(1-2m')} \log\left\{1 + \frac{(1-2m')(2-m')}{3} \log r'\right\}\right]. \quad (12.10)$$

The use of (12.6) now yields the values of h/h_o in terms of r along the line LM'. The relations according to the equations (12.6) through (12.10) are plotted in Figures 14 and 15 for values of r from 0.46337 to 1. The comparison shows that the above procedure gives results that are practically identical with those of the von Mises theory.

If the penetration of the tube is small, such as $0.6 \leq r \leq 1$, only one linear linearised yield locus LM' is needed.

For setting σ_1/σ_o = -0.57735, and r_1 = 0.6, the equation (10.3) gives

$$r(M') = 1.06878$$

so that the linear yield locus LM' covers the entire range $1 \leq r \leq 0.6$. Rather setting σ_1/σ_o = -0.57735 and r=1, the equation (10.3) yields

$$r_1 = 0.56138$$

so that for penetrations of the range $0.56138 \leq r \leq 1$, the single linear yield locus LM' is sufficient to give good results.

Discussion.

The Figures 3 to 8, and 10 to 15 show that in both problems, drawing of tubes and nosing of shells, the modified linearised procedure closely approximates the results of the von Mises theory. A single linear yield condition is suitable only if the changes in diameter are small. In all other cases two or more linear yield conditions must be used. The linearised procedure then gives continuous stresses, thicknesses, and velocities, but discontinuous first derivatives. In the modified linearised procedure these discontinuities do not appear.

Bibliography

[1] H. Tresca, Comptes Rendus, Acad. Sci. Paris, 59(1864)754.

[2] R. von Mises, Z. Angew. Math. Mech. 8(1928)161.

[3] M. Lèvy, Comptes Rendus, Acad. Sci. Paris, 70(1870)1323.

[4] W. Prager, "An Introduction to Plasticity," Addison-Wesley, Reading, Mass., 1959, p.37.

[5] P.G. Hodge,Jr., J. Appl. Mech., 20(1953)183.

[6] H.W. Swift, Phil. Mag. 40(1949)883.

[7] R. von Mises, Gottinger Nachrichten, Math.-phys. Klasse (1913)582.

[8] W. Prager, Proc. Instn. Mech. Engrs. 169(1955)41.

[9] V.V. Sokolovskii, Prikl. Mat. Mekh. 25(1961)931.

[10] E.T. Onat and W. Prager, Brown University, Technical Report DA798/15 (1954).

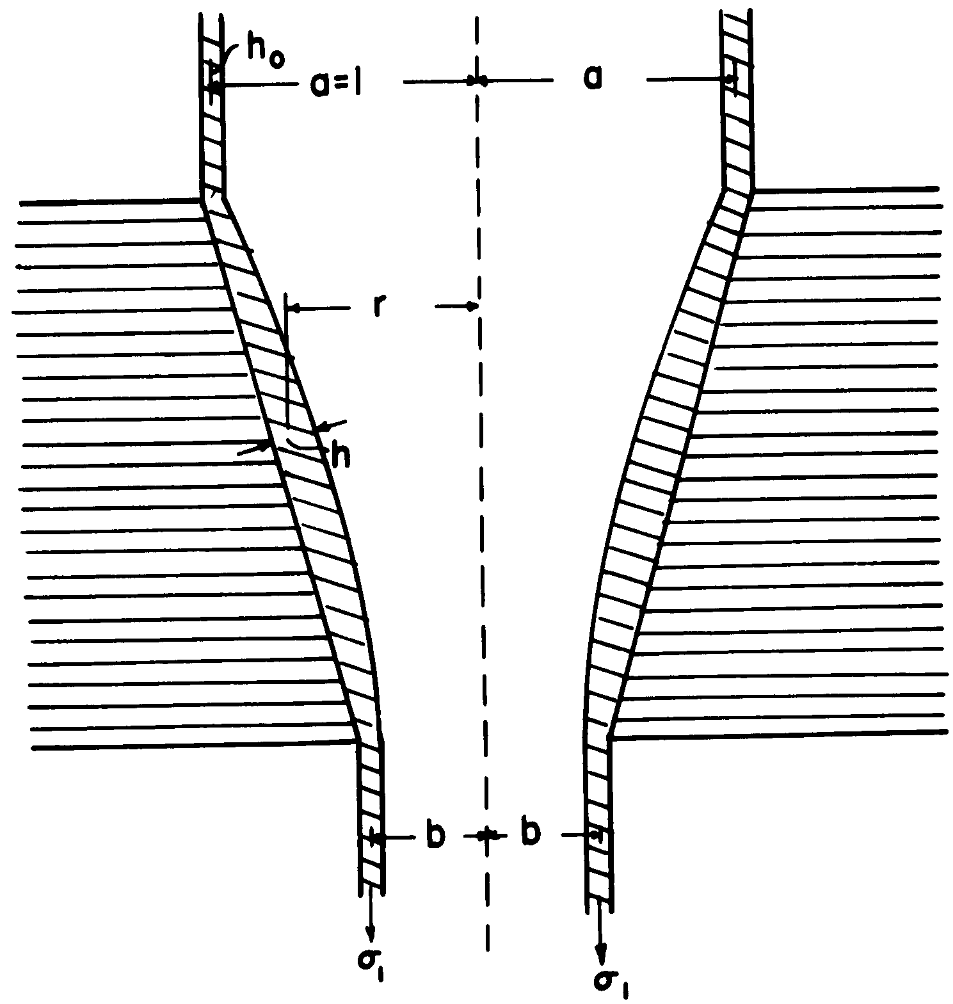

FIG. 1

h_o: initial thickness

h: thickness of tube at radius r

b: radius of tube at die exit

a: radius of tube at die entrance, taken as unit of length

σ_1: meridional stress

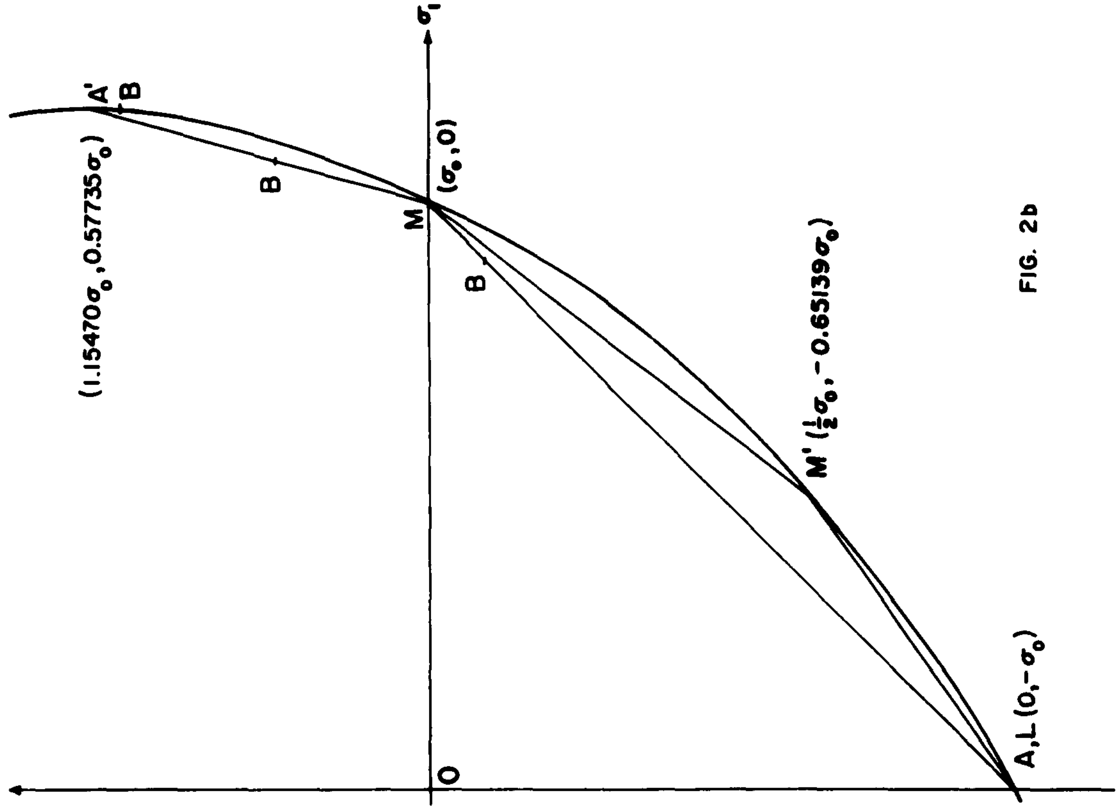
σ1
A'
B
(1.15470σ0, 0.57735σ0)
B
M
(σ0, 0)
B
M' (½σ0, -0.65139σ0)
A, L (0, -σ0)
O

FIG. 2b

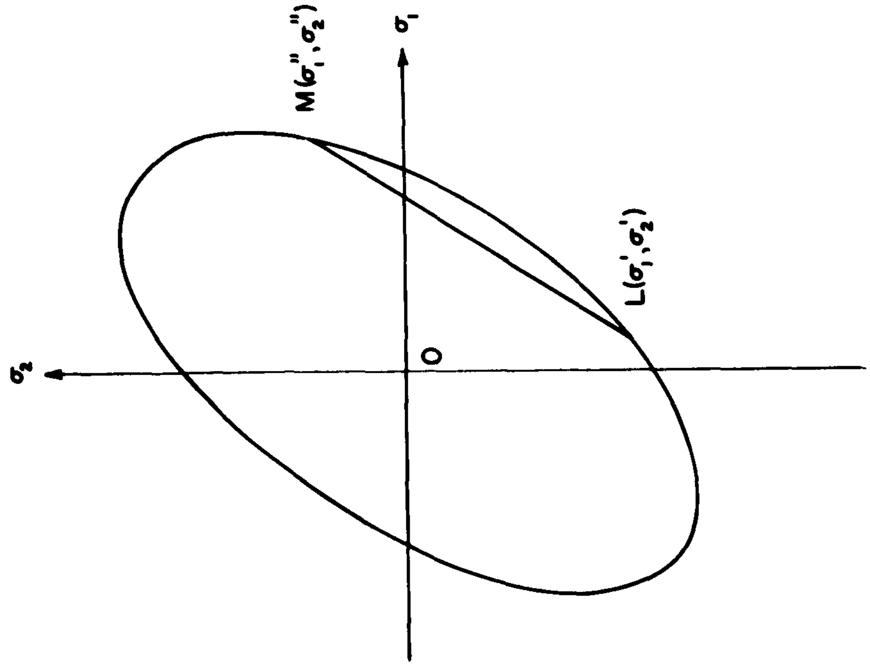
σ1
M(σ1'', σ2'')
L(σ1', σ2')
O
σ2

FIG. 2a

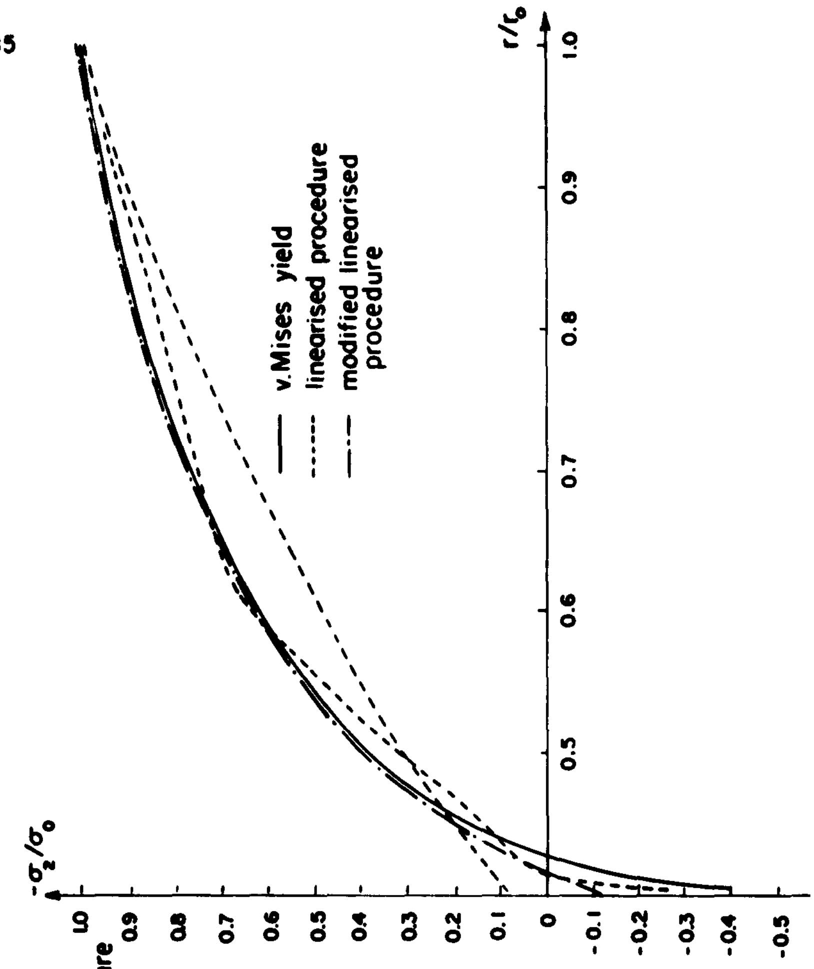
$-\sigma_2/\sigma_0$
r/r_0
v. Mises yield
linearised procedure
modified linearised procedure
1.0
0.9
0.8
0.7
0.6
0.5
0.4
0.3
0.2
0.1
0
-0.1
-0.2
-0.3
-0.4
-0.5

FIG. 4

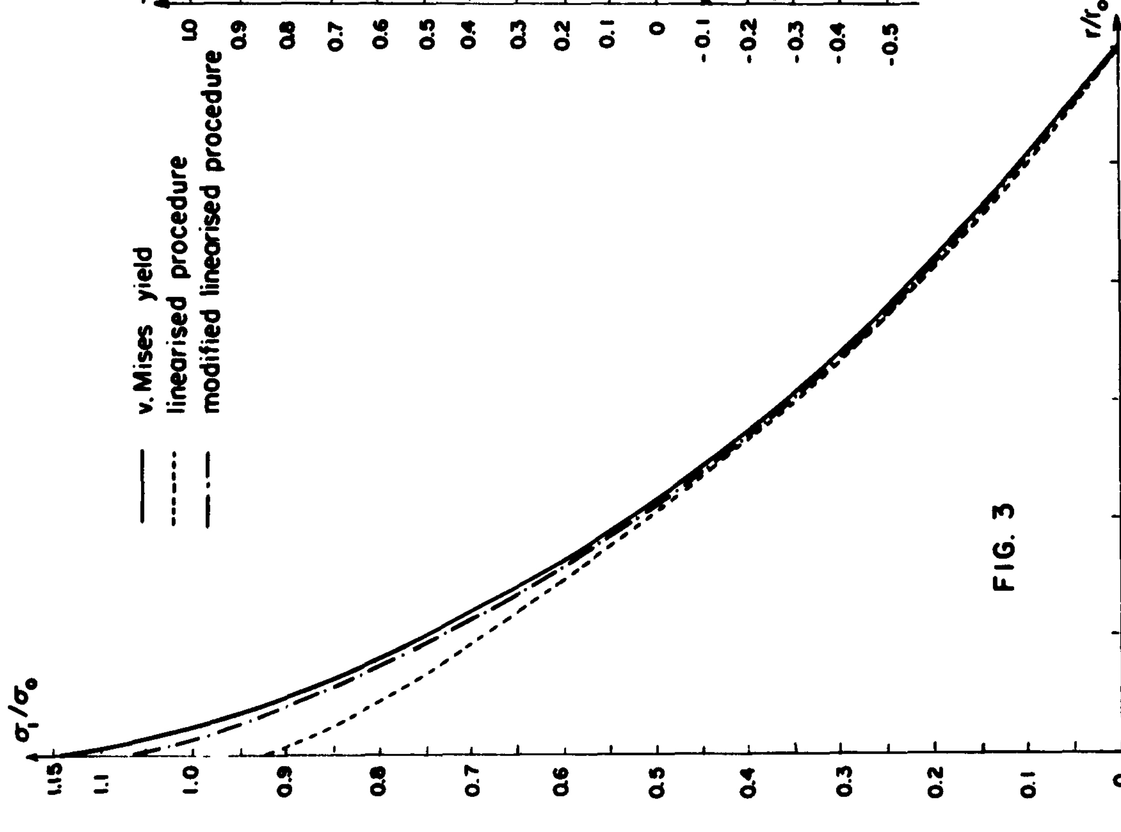
σ_1/σ_0
r/r_0
v. Mises yield
linearised procedure
modified linearised procedure
1.15
1.1
1.0
0.9
0.8
0.7
0.6
0.5
0.4
0.3
0.2
0.1
0

FIG. 3

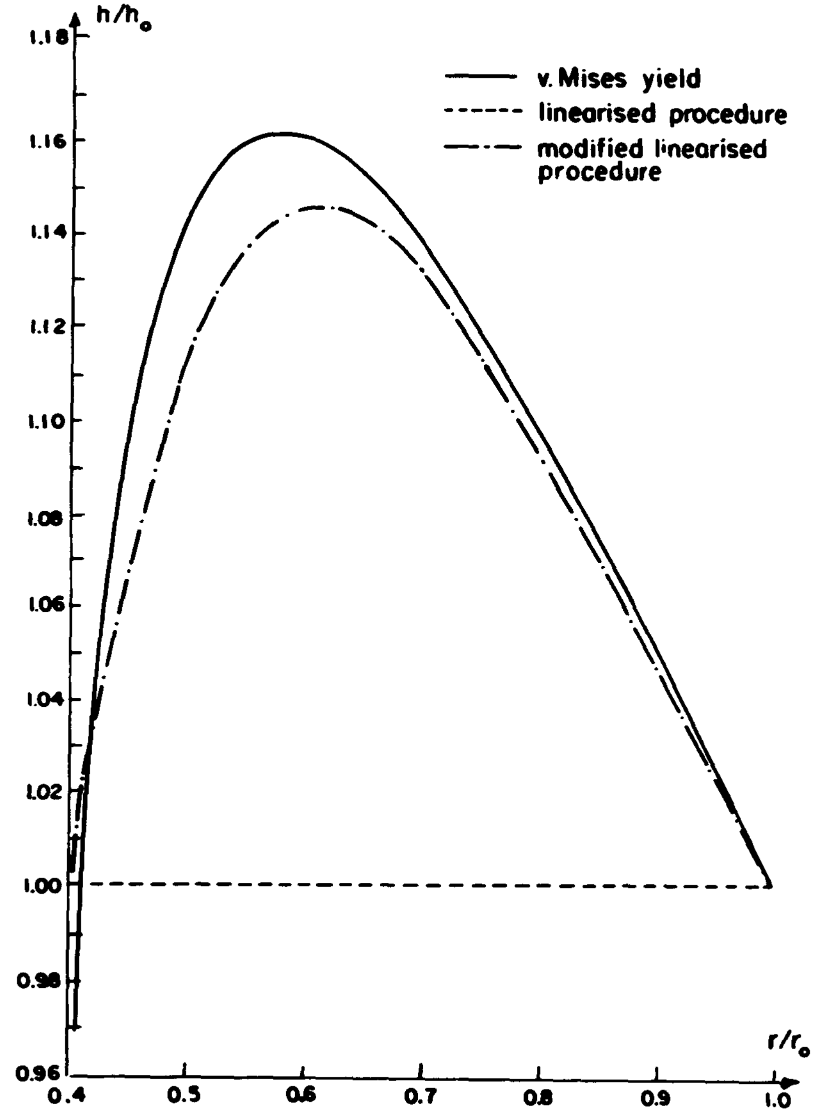
h/h₀
1.18
1.16
1.14
1.12
1.10
1.08
1.06
1.04
1.02
1.00
0.98
0.96
0.4
0.5
0.6
0.7
0.8
0.9
1.0
r/r₀
v. Mises yield
linearised procedure
modified linearised procedure

FIG. 5

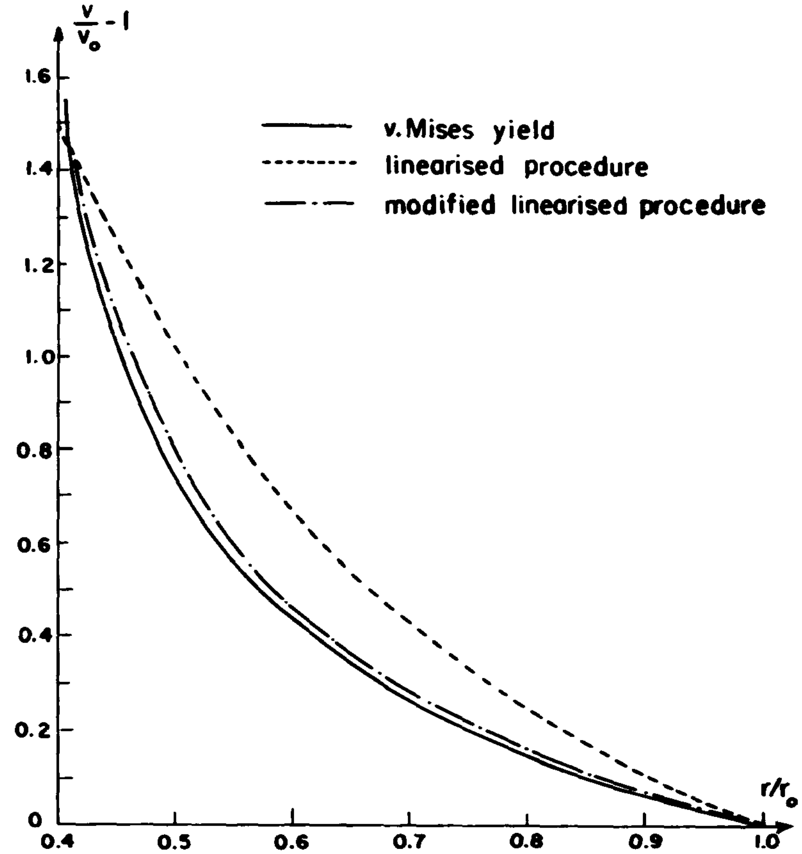
v/v₀ - 1
1.6
1.4
1.2
1.0
0.8
0.6
0.4
0.2
0
0.4
0.5
0.6
0.7
0.8
0.9
1.0
r/r₀
v. Mises yield
linearised procedure
modified linearised procedure

FIG. 6

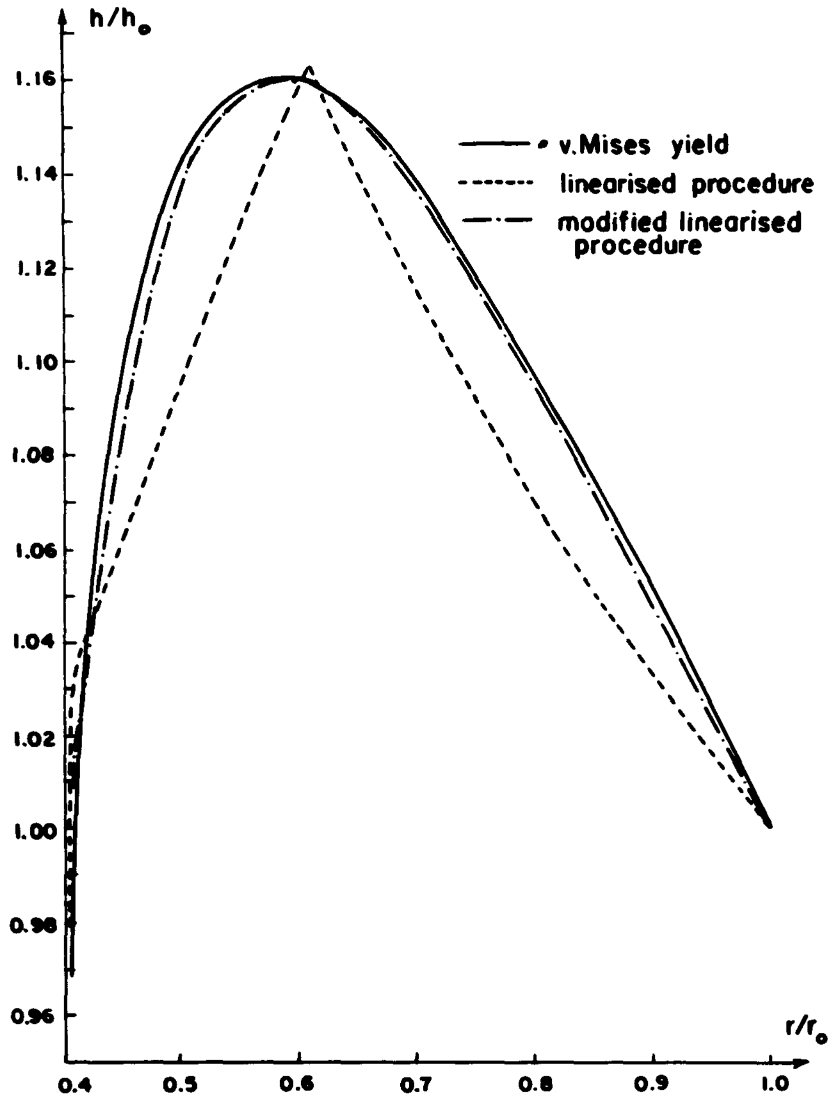
h/h₀
v.Mises yield
linearised procedure
modified linearised procedure
r/r₀
1.16
1.14
1.12
1.10
1.08
1.06
1.04
1.02
1.00
0.98
0.96
0.4
0.5
0.6
0.7
0.8
0.9
1.0

FIG. 7

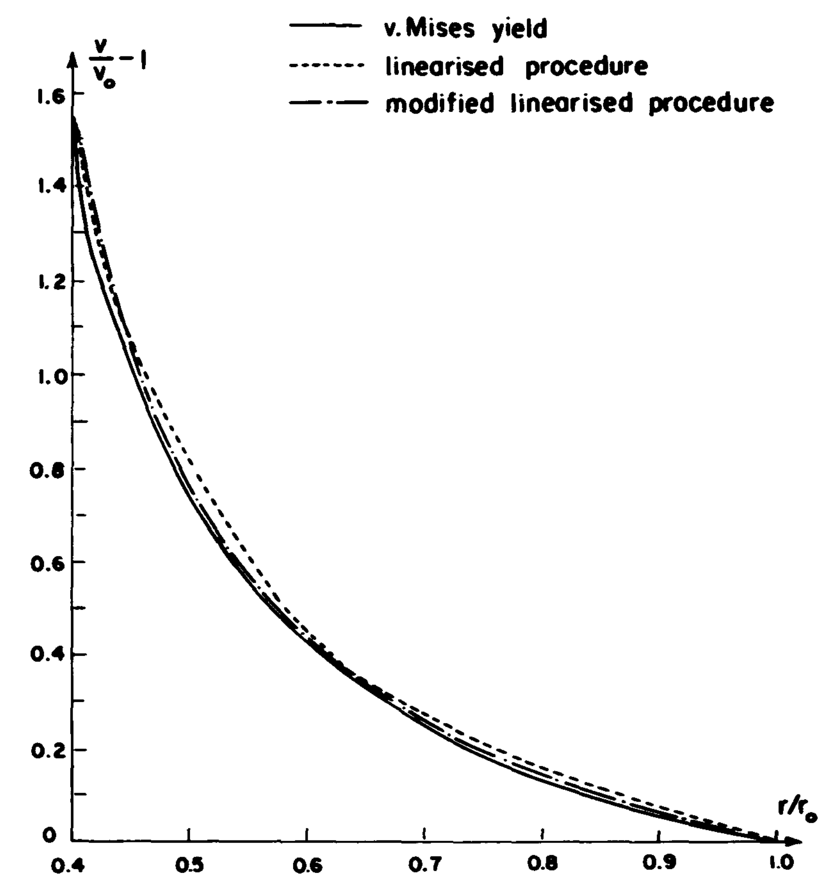
v/v₀ - 1
v.Mises yield
linearised procedure
modified linearised procedure
r/r₀
1.6
1.4
1.2
1.0
0.8
0.6
0.4
0.2
0
0.4
0.5
0.6
0.7
0.8
0.9
1.0

FIG. 8

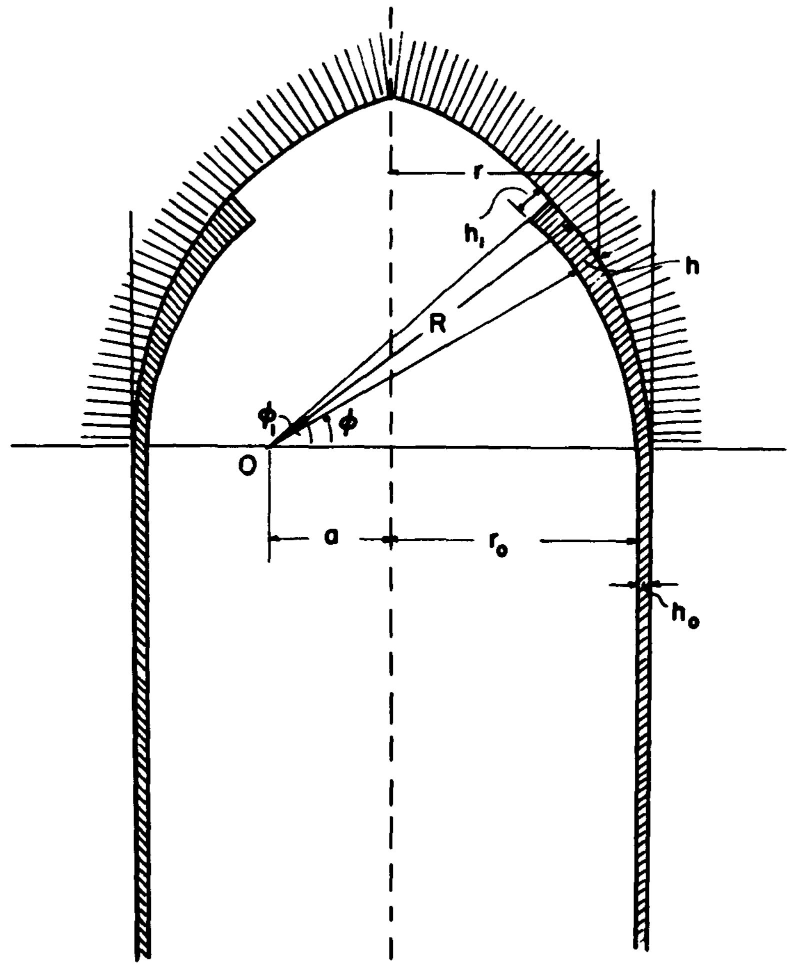
r
h_1
h
R
ϕ_1
ϕ
O
a
r_0
h_0

FIG. 9a

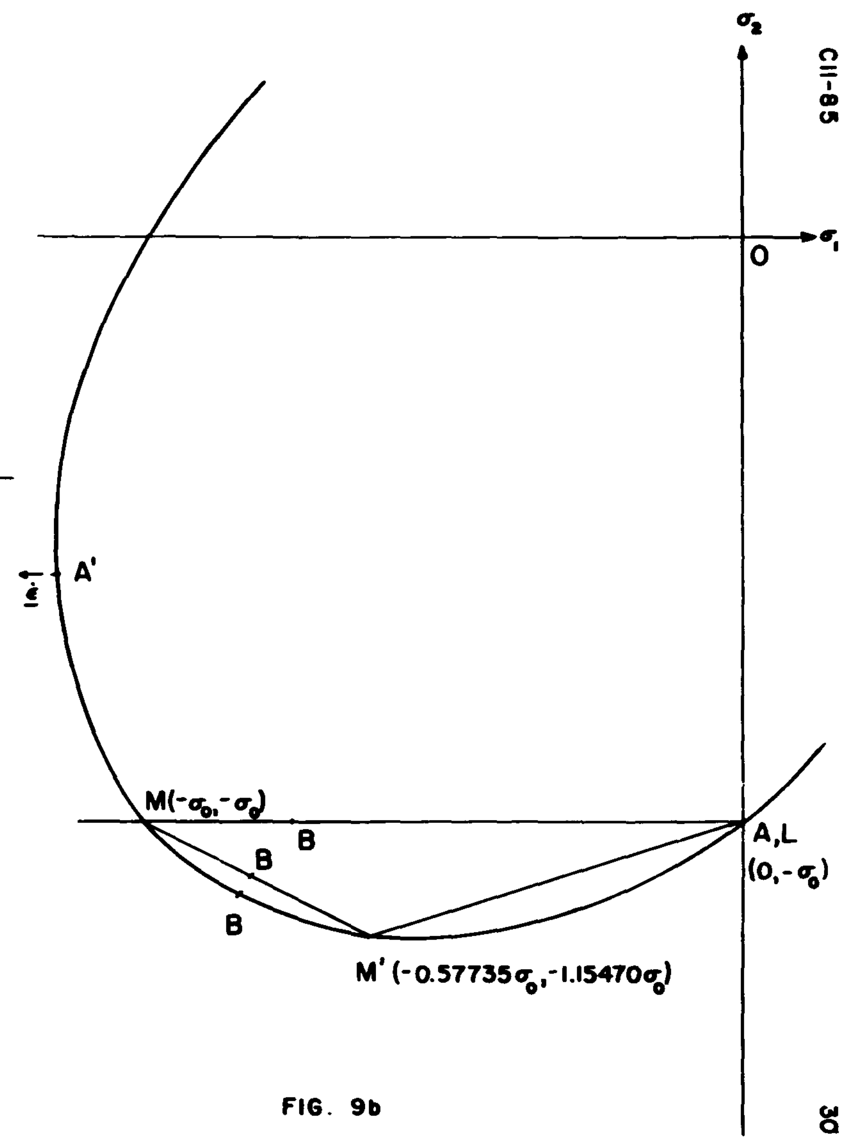
σ_2
σ_1
O
A'
$\dot{\epsilon}$
M($-\sigma_0$, $-\sigma_0$)
B
B
B
A,L
(0, $-\sigma_0$)
M' ($-0.57735\sigma_0$, $-1.15470\sigma_0$)

FIG. 9b

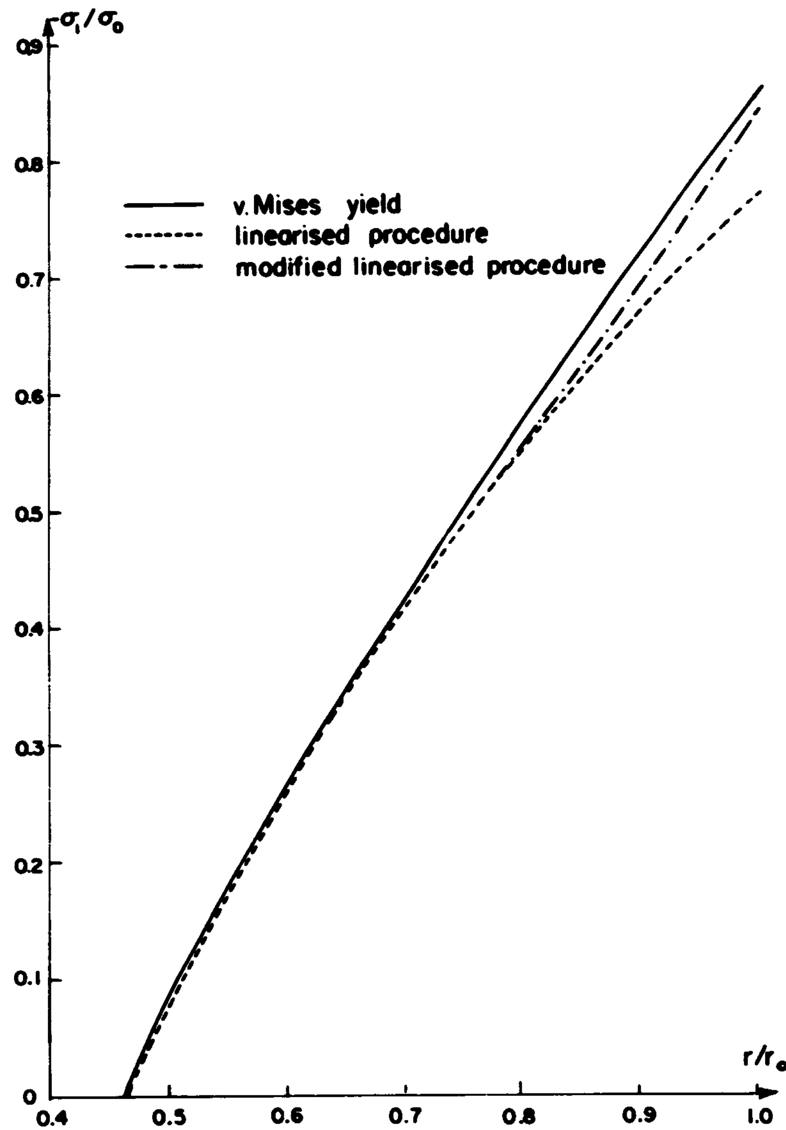
$-\sigma_1/\sigma_0$
0.9
0.8
0.7
0.6
0.5
0.4
0.3
0.2
0.1
0
0.4
0.5
0.6
0.7
0.8
0.9
1.0
r/r_0
v. Mises yield
linearised procedure
modified linearised procedure

FIG. 10

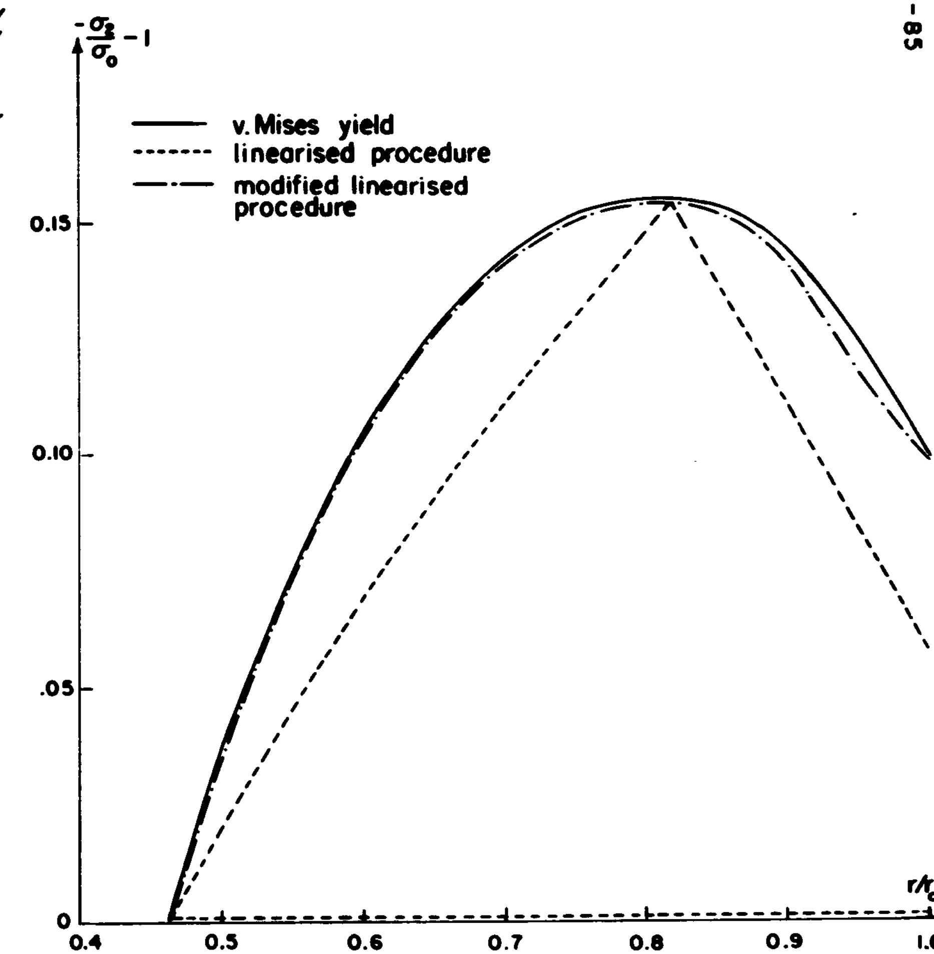
$-\frac{\sigma_2}{\sigma_0}-1$
0.15
0.10
.05
0
0.4
0.5
0.6
0.7
0.8
0.9
1.0
r/r_0
v. Mises yield
linearised procedure
modified linearised procedure

FIG. 11

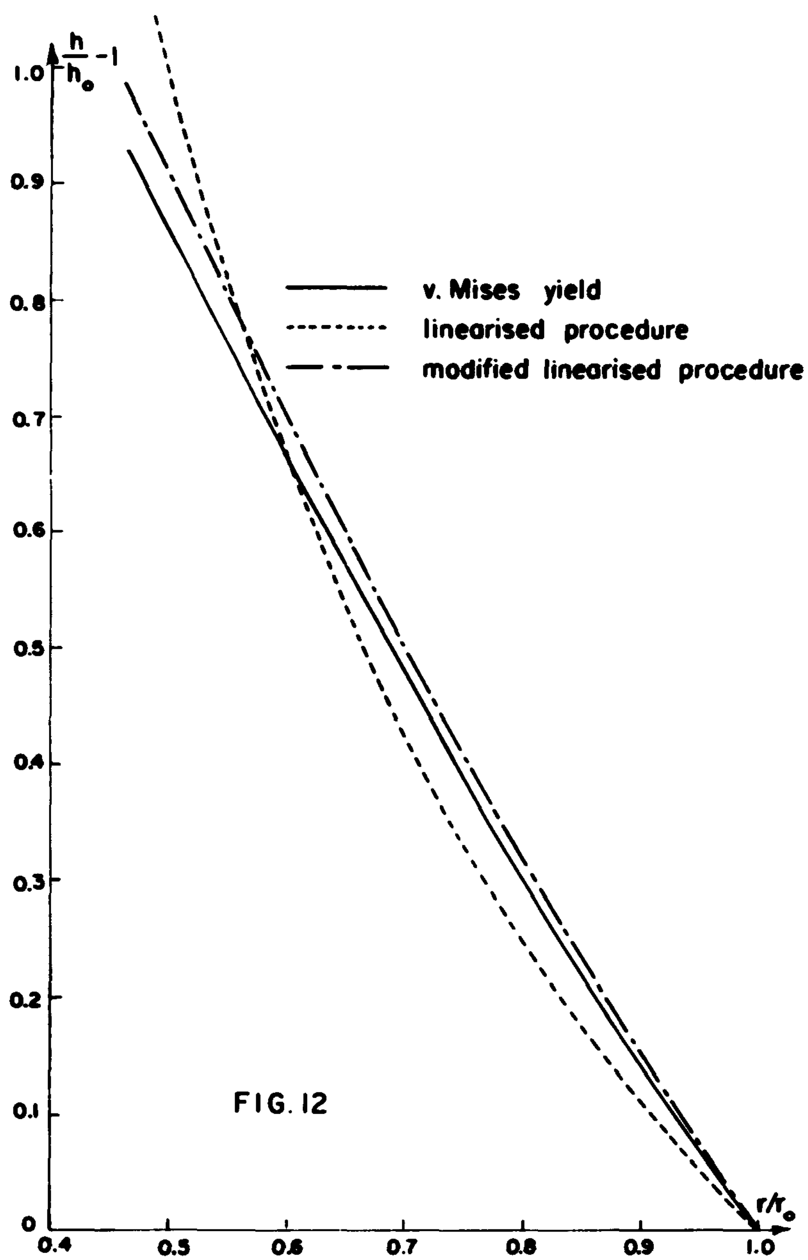
$\frac{h}{h_o}-1$
1.0
0.9
0.8
0.7
0.6
0.5
0.4
0.3
0.2
0.1
0
0.4
0.5
0.6
0.7
0.8
0.9
1.0
r/r_o
v. Mises yield
linearised procedure
modified linearised procedure

FIG. 12

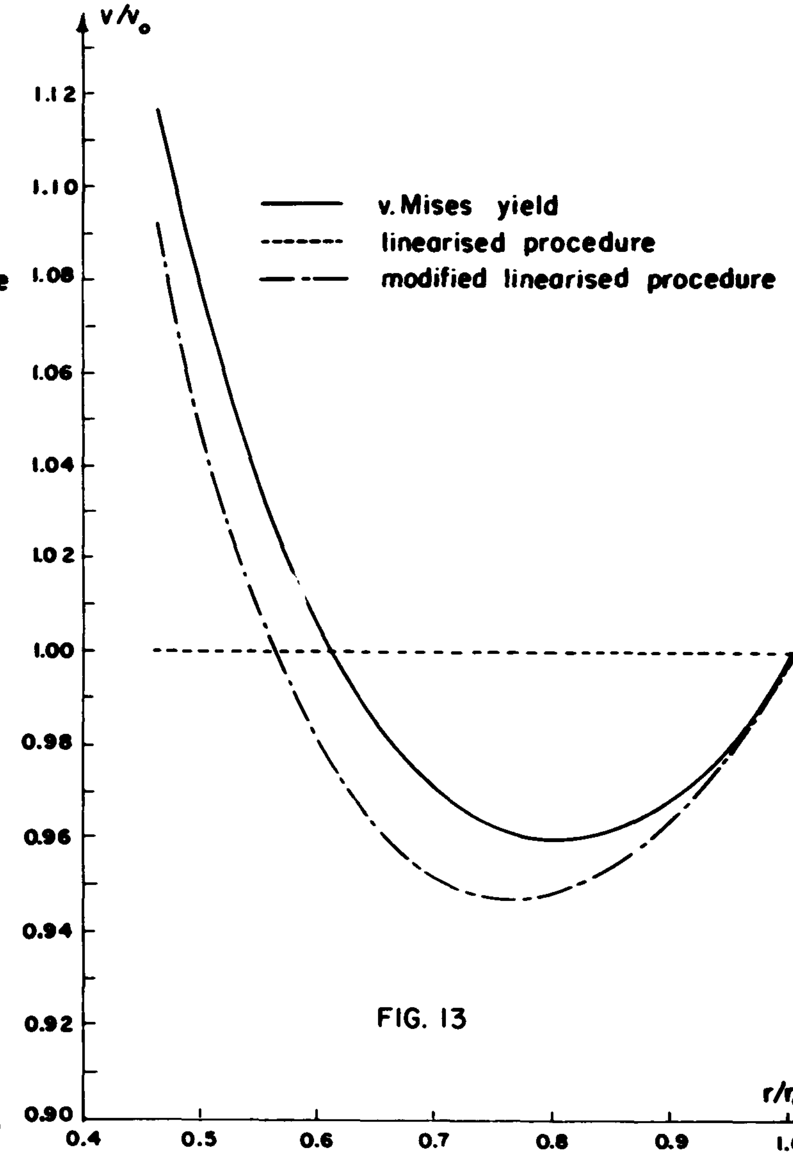
v/v_o
1.12
1.10
1.08
1.06
1.04
1.02
1.00
0.98
0.96
0.94
0.92
0.90
0.4
0.5
0.6
0.7
0.8
0.9
1.0
r/r_o
v. Mises yield
linearised procedure
modified linearised procedure

FIG. 13

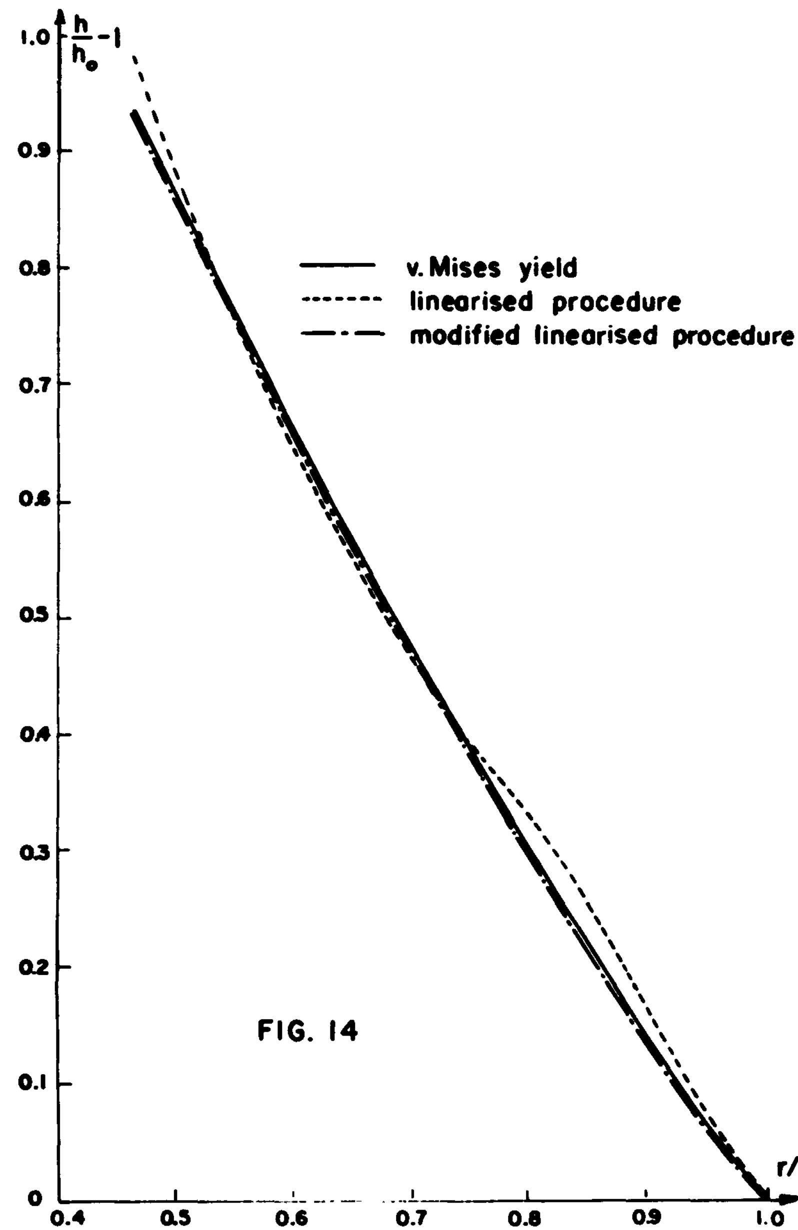

$\frac{h}{h_o}-1$
1.0
0.9
0.8
0.7
0.6
0.5
0.4
0.3
0.2
0.1
0
0.4
0.5
0.6
0.7
0.8
0.9
1.0
r/r_o
v. Mises yield
linearised procedure
modified linearised procedure

FIG. 14

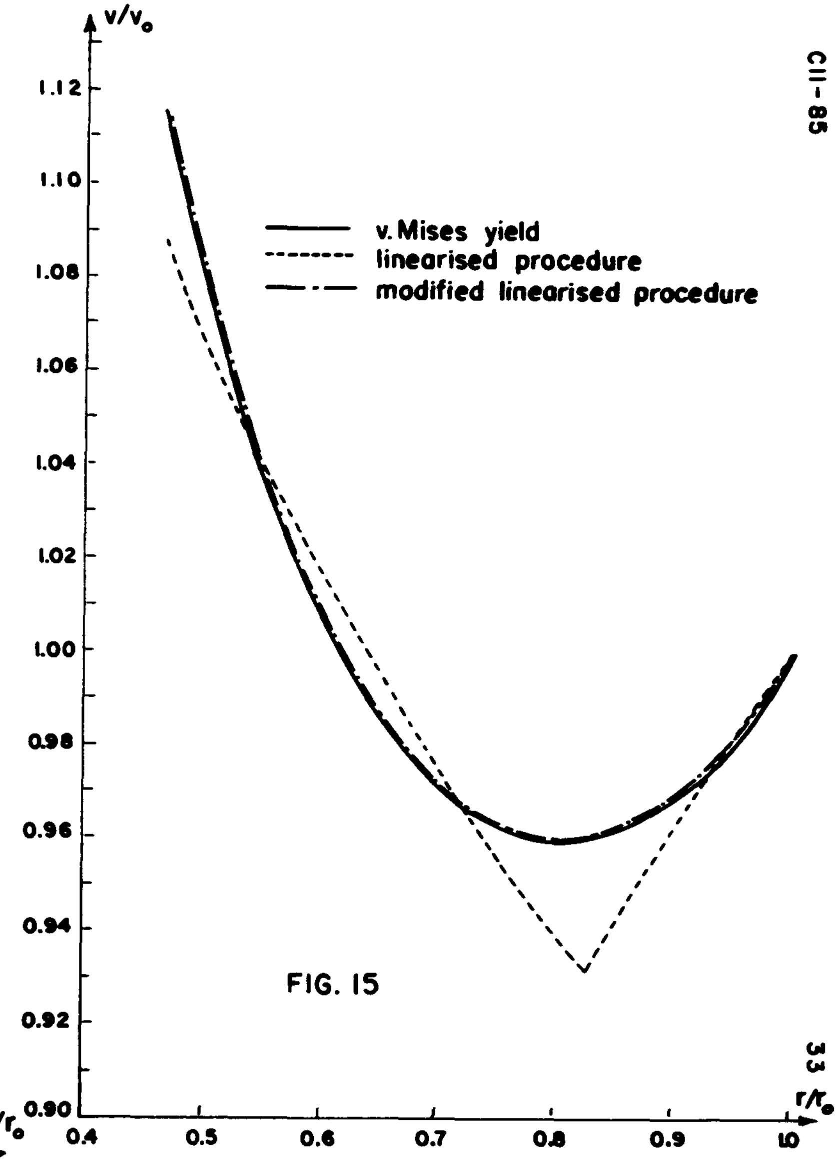

v/v_o
1.12
1.10
1.08
1.06
1.04
1.02
1.00
0.98
0.96
0.94
0.92
0.90
0.4
0.5
0.6
0.7
0.8
0.9
1.0
r/r_o
v. Mises yield
linearised procedure
modified linearised procedure

FIG. 15